heritage

MDPI

*Article*

# Archaeometric Investigation of Artificial Stone Materials from the *Theatrum Marcelli* (Rome, Italy)

**Maria Aantonietta Zicarelli [1], Michela Ricca [1,*], Maria Francesca Alberghina [1,2], Salvatore Schiavone [2], Mauro Francesco La Russa [1,*] and Luciana Randazzo [3,4]**

[1] Department of Biology, Ecology and Earth Sciences (DiBEST), University of Calabria, Via Bucci, 87036 Arcavacata di Rende, Italy; mariaantonietta.zicarelli@unical.it (M.A.Z.); maria.alberghina@unical.it (M.F.A.)
[2] S.T.Art-Test di S. Schiavone & C Sas, 88 Via Stovigliai, 93015 Niscemi, Italy; info@start-test.it
[3] Department of Earth and Marine Sciences (DiSTeM), University of Palermo, 26 Via Archirafi, 90123 Palermo, Italy; luciana.randazzo@unipa.it
[4] Istituto Nazionale di Geofisica e Vulcanologia, Sezione di Palermo, Via Ugo la Malfa, 90146 Palermo, Italy
* Correspodence: michela.ricca@unical.it (M.R.); mlarussa@unical.it (M.F.L.R.)

**Abstract:** This study illustrates the results of minero-petrographic and microchemical investigations of artificial stone materials (mortars, plasters, and bricks) taken from the *Theatrum Marcelli* (Rome, Italy). To achieve this objective, the artificial building materials were analysed using Polarized Optical Microscopy (POM) and a Scanning Electron Microscope (SEM) used in backscattered electron (BSE) mode and coupled with an Energy-Dispersive Spectrometer (EDS) after a sampling campaign. The POM was aimed at collecting information on the textural and mineralogical characteristics of the samples (identification of the main minerals constituting the aggregate, grain size and shape, and the evaluation of the binder/aggregate ratio). The data also supported technological assessments through the characterization of the raw materials used for the manufacture of the mortars/plasters. Furthermore, the SEM-EDS investigations revealed the chemical composition of both the aggregate and the binder, which was useful for estimating their hydraulicity index (HI). The diagnostic campaign allowed us to obtain interesting information on the plasters/mortars used in the *Theatrum Marcelli*, together with their probable production technology. In particular, the raw materials were quite homogeneous, thus confirming the traditional methodology used in Roman times to create natural hydraulic mortars by the addition of pozzolanic volcanic material to aerial lime. The volcanic component of the aggregate seems to be compatible with the ultrapotassic products of the Roman Magmatic Province—likely with the *Pozzolane Rosse* pyroclastic deposit of the Alban Hills district.

**Keywords:** *Theatrum Marcelli*; hydraulic mortar; hydraulicity index; pozzolana; brick; plaster; Roman mortar technology; petrography analyses; SEM-EDS investigations

Academic Editor: Rafael Fort González

Received: 5 December 2024
Revised: 8 January 2025
Accepted: 30 January 2025
Published: 31 January 2025

**Citation:** Zicarelli, M.A.; Ricca, M.; Alberghina, M.F.; Schiavone, S.; La Russa, M.F.; Randazzo, L. Archaeometric Investigation of Artificial Stone Materials from the *Theatrum Marcelli* (Rome, Italy). *Heritage* **2025**, *8*, 57. https://doi.org/10.3390/heritage8020057



## 1. Introduction

The use of construction materials in Roman architecture demonstrates extraordinary engineering ability, based on the knowledge and expertise of builders who reworked local materials to achieve durable complex stone and concrete masonry [1]. Monuments from the Republican era and the early Imperial period are the result of the skilful use of diverse volcanic deposits from the nearby Monti Sabatini and Colli Albani districts, as well as travertine quarried near Tivoli [2].

The employment of different materials reflects the progressive technological evolution that, over time, allowed increasingly complex and refined engineering solutions. Archaeological evidence indicates that the earliest Republican monuments in Rome were constructed using the soft volcanic tuffs immediately available locally on Palatine Hill. It was only from the 1st century BCE, with the acquisition of nearby territories, that more durable and well-lithified tuffs, sourced from the Monti Sabatini and Albani volcanic districts, were quarried to obtain dimension stone for *opus quadratum* masonries. Travertine blocks decorated the tuff walls as keystones, capitals, or facing slabs, as seen in the Forum of Caesar (46 BCE) [3,4]. By the late Republican period, Roman builders introduced a significant technological shift. Walls began to be constructed with a concrete core (*opus caementicium*) and were faced with tuff blocks arranged in irregular and geometric patterns (*opus incertum* and *opus reticulatum*, respectively) or fired bricks (*lateres cocti*), as in *opus testaceum*.

This technical know-how extended beyond the selection of cut stone elements, including advanced techniques for preparing pozzolanic mortars to enhance their strength and durability [5–9]. Scientific studies of Roman mortars reveal that in the early stages (beginning of the 2nd century BCE), they contained crushed tuff as fine and coarse aggregate, alongside less coherent pyroclastic deposits sourced from nearby outcrops close to construction sites. This suggests an initial lack of a standardized system for selecting pozzolanic materials, prioritizing proximity to extraction sites and ease of availability. It was from the late 2nd to early 1st century BCE that builders realized the potential of adding pozzolanic aggregates from specific altered facies to significantly improve the mechanical properties of mortars. From the Augustan age onwards, systematic selection became common, both in the construction of new complex buildings and in restoration interventions on older structures [10–13].

These findings are supported by ancient sources, particularly Vitruvius's *De Architectura*, written between 31 and 27 BCE, during the transition between the late Republican and early Imperial period. In his work, Vitruvius provides detailed documentation on how Republican builders carefully selected various volcanic and sedimentary stones available in the Roman region, taking into account their durability and stability under diverse environmental conditions. The builders' ability to adapt these materials to specific construction needs highlights a deep understanding of their physical and mechanical properties, supported by a combination of practical experience (*fabrica*) and theoretical reflection (*ratiocinatione*), a synthesis Vitruvius himself celebrates as "*scientia*" [14].

Thus, the builders of the late Republican era inherited and refined a wealth of skills rooted in meticulous observation, extensive practical experience, and innovative experimentation. This foundation enabled them to achieve remarkable technical advances that would come to define Roman imperial architecture. The need to innovate was also driven by constant environmental challenges, such as frequent floods of the Tiber, earthquakes, and fires, which required resilient architectural solutions [2,15–17]. Additionally, military conquests and the growing wealth of the Republic encouraged a culture of patronage and competition among the elite, who used monumental architecture to express their prestige. These dynamics led to a "race for innovation" in the design and execution of more complex buildings requiring increasingly advanced techniques.

The Theatre of Marcellus (30?—11 BCE) stands as one of the monuments embodying the technological advancements of the transition from the late Republican to the Imperial period, born from the fortune of Emperor Augustus's elaborate building and restoration program.

## 2. Historical Background and Building Materials of the *Theatrum Marcelli*

The *Theatrum Marcelli* was built by Emperor Augustus *ad aedem Apollonis* in the Campus Martius area, a site designated since the Republican period for theatrical *ludi* [18] (Figure 1).

It remains uncertain whether the theatre was constructed based on a pre-existing design by Julius Caesar. However, it is rather clear that Caesar initiated the preparation of the area, as he had planned to build a vast theatre sloping down from the *Rupe Tarpea* (*Theatrum summae magnitudinis Tarpeio monti accubans*) [19]. The area of the *Circus Flaminius*, designated for the theatre's construction, was already densely populated and occupied by civil and religious buildings, including the *Circus Flaminius* itself, the *Porticus Metelli*, the Temples of *Apollo Medicus* and *Bellona*, and the temples of the *Forum Holitorium* (Figure 1a). For this reason, it was necessary to demolish a substantial portion of the existing structures, while the sacred buildings were either relocated or restored. An exception was made only for the Temple of *Pietas*, which was never rebuilt, a decision for which Caesar faced significant criticism [20].

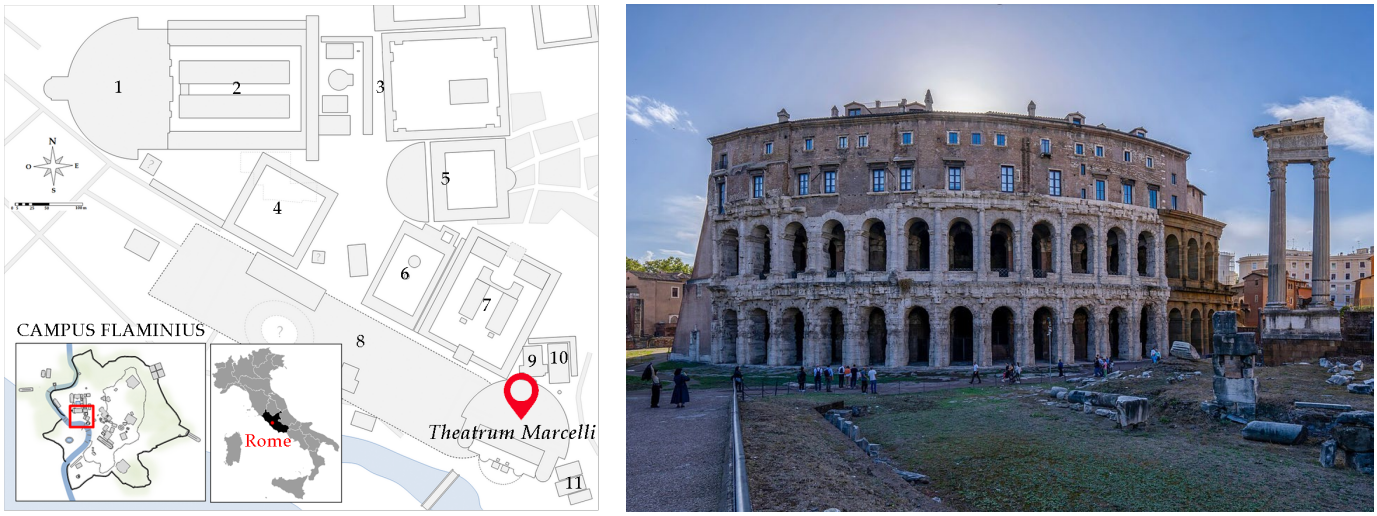


(**a**) (**b**)

**Figure 1.** (**a**) Map of *Campus Flaminius* area in Rome in which the *Theatrum Marcelli* (red square) and some other important monuments are located: *Theatrum Pompeii* (1); *Porticus Pompeii* (2); *Porticus Minucia* (3); *Porticus Octavia* (4); *Theatrum Balbi* and *Crypta Balbi* (5); *Porticus Philippi* (6); *Porticus Octaviae* (ex *Porticus Metelli*) (7); *Circus Flaminius* (8); Temple of *Apollo Medicus* (9); Temples of *Bellona* (10); Temples of the *Forum Holitorium* (11) (image modified and reproduced under Creative Commons Attribution-ShareAlike 4.0 International license—Cassius Ahenobarbus author (https://it.wikipedia.org/wiki/Regio_IX_Circus_Flaminius#/media/File:Plan_champ_de_mars_sud.png (accessed on 25 November 2024)), "Plan champ de mars sud"). (**b**) Overall view of *Theatrum Marcelli* (image reproduced under Creative Commons Attribution-ShareAlike 4.0 International license—Fiat 500e author (https://en.wikipedia.org/wiki/Theatre_of_Marcellus#/media/File:Teatro_di_Marcello_intero.jpg (accessed on 25 November 2024)), "Teatro di Marcello intero").

Thus, the construction process can be divided into two distinct phases: the initial clearance of the area by Caesar, followed by the theatre's erection under Augustus, who acquired additional private lands at his own expense [18].

Augustus, therefore, ordered the levelling and paving of the area, standardizing the elevation across the entire space between the *Porticus Octaviae* and the *Forum Holitorium*. Given that the new Temple of *Apollo Sosianus* and the *Porticus Octaviae* date between 30

and 20 BCE, and considering the chronological alignment with these structures, the *Theatrum Marcelli* may have been constructed within this same time frame [20]. The theatre was dedicated to the memory of Augustus's nephew, Marcellus, the son of his sister Octavia and husband of his daughter Julia, who had been destined for succession but died prematurely in 23 BCE [21]. In 17 BCE, the structure, likely still incomplete, hosted the *ludi seculares*, but the formal inauguration took place most probably in 13 BCE [21]. After Nero's fire and the battle of the Capitoline by Vitellius' forces in 69 CE, Vespasian restored the theatre's *scena*, and further renovations likely occurred under Alexander Severus [22], though additional details are scarce.

The theatre likely remained in use at least until the end of the 5th century CE. Despite some of the theatre travertine blocks being removed and used for the restoration of the *Pons Cestius* at the end of the 4th century, new statues were commissioned for the theatre in 421 CE by the prefect Petronius Maximus [23]. Over the centuries, however, the structure suffered from various modifications and natural disasters, such as earthquakes and Tiber floods, which caused the significant burial and collapse of some areas of the theatre [16,17].

In the 12th century, the building came under the control of the Faffi family, who converted it into a fortified structure [24]. In the 16th century, the Savelli family transformed the theatre into a palace, based on a design by Baldassare Peruzzi, and it was later acquired by the Orsini in the 18th century. The theatre was finally cleared of additions in the 1920s when it was acquired by the City of Rome [20].

The *Theatrum Marcelli* is among the best-preserved ancient Roman theatres. Its design appears to have been conceived as a political and urban response to the older Theatre of Pompey [23]. The *Theatrum Marcelli* was the second largest in terms of size, with a capacity of about 20,550 *loca* (around 15,000 spectators) compared to the 17,580 seats of the Theatre of Pompey [25].

Today, elements of the original structure that remain identifiable include the facade with two of the three ambulacra (Doric and Ionic), two internal galleries known as the "Knights' Gallery" (*ambulacro dei Cavalieri*), and the "Upper Small Ambulatory" (*piccolo ambulacro superiore*), which helped direct the flow of spectators within the building (Figures 1 and 2) [20]. There are also several internal rooms originally used as storage spaces and shops, along with elongated *fornici*. Due to the complexity of the structure, different construction techniques and materials were used to meet the architectural and structural requirements. Materials such as travertine and tuff were employed for the load-bearing sections, which were subjected to greater mechanical stress [20]. The facade was built in *opus quadratum* of travertine, while the counter-façade and parts of the radial walls were constructed with *opus quadratum* in *tufo lionato*, incorporating travertine for the keystones and impost blocks. In contrast, the inner walls were made with *opus caementicium* and faced with *opus reticulatum* and bricks (*opus testaceum*). *Opus testaceum* was utilized exclusively for the internal semi-annular *ambulacra*. Moreover, the walls of the *ambulacro dei Cavalieri* were constructed using two distinct techniques: the inner wall, adjacent to the orchestra, was faced with uniform yellow bricks, while the opposing wall was made with *opus reticulatum* (Figure 2) [26].

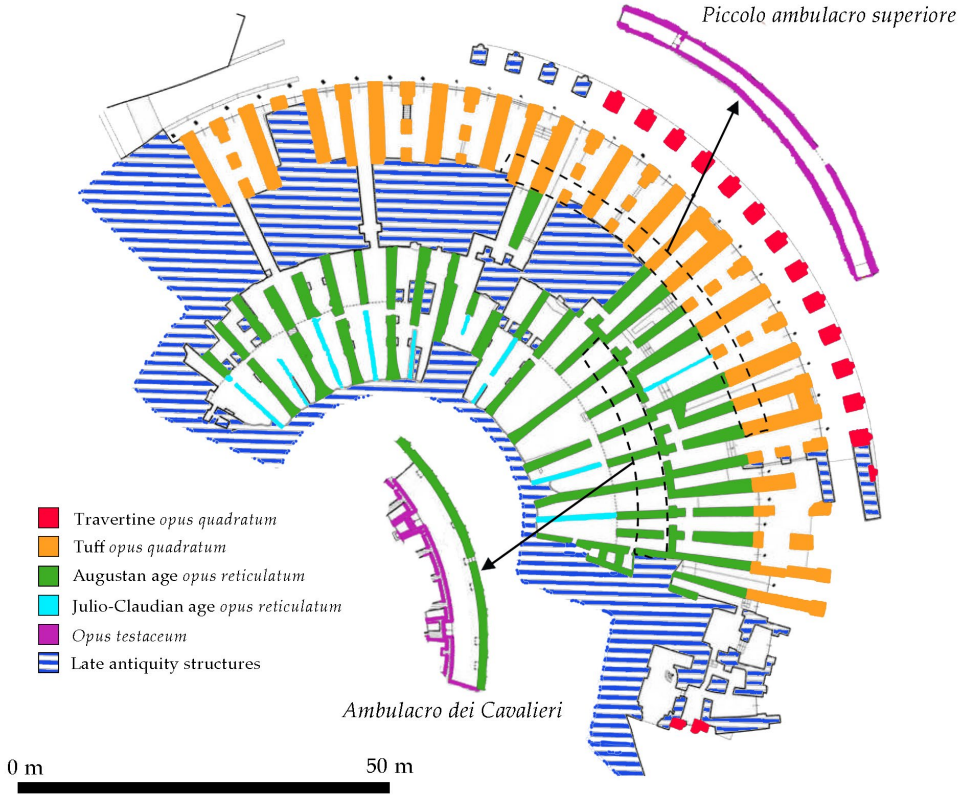


**Figure 2.** Ground floor plan of the *Theatrum Marcelli*, showing the *Ambulacro dei Cavalieri* and the *Piccolo ambulacro superiore*, along with the corresponding masonry techniques and building materials used in the monument construction, modified from Rossetto and Buonfiglio, 2010 [20].

This paper aims to characterize the different building materials used in the construction of the *Theatrum Marcelli*. In particular, the layers of some plasters, mortars, and bricks taken from diverse areas of the monument are investigated. The purpose is to improve knowledge about the Roman construction techniques used for the production of artificial stone materials in the early years of the Empire, and thus confirm the shift toward a more conscious and developed know-how. A diagnostic campaign was addressed to define the minero-petrographic and chemical features of the investigated materials, taking into account compositional analogies and differences among the samples under analysis.

## 3. Materials and Methods

A total of 10 samples of different artificial stone materials were collected from diverse areas of the *Theatrum Marcelli*. Sampling was conducted with criteria such as maximum representativeness and minimal invasiveness, using the most appropriate stainless-steel tools (e.g., lancets and small chisels). A comprehensive list of the samples, including material types and descriptions of the sampling points, is provided in Table 1.

**Table 1.** List of the analysed samples and descriptions of the sampling locations and types of materials.

| Sample ID | Sampling Location | Description |
|---|---|---|
| TM_1 | *Ambulacro dei Cavalieri (fornice 4)* | Mortar (*opus testaceum*) |
| TM_2 | *Ambulacro dei Cavalieri (fornice 4)* | Yellow brick |
| TM_3 | *Ambulacro dei Cavalieri (fornice 4)* | Mortar (*opus reticolatum*) |

| | | |
|---|---|---|
| TM_4 | *Ambulacro dei Cavalieri (fornice 4)* | Mortar |
| TM_5 | *Ambulacro dei Cavalieri (fornice 4)* | Three-layer plaster |
| TM_6 | *Fornice 10* | Mortar (*opus reticolatum*), external coating |
| TM_7 | *Fornice 10* | Mortar (*opus reticolatum*), internal wall |
| TM_8 | *Fornice 12* | Mortar (*opus reticolatum*), central wall |
| TM_9 | *Fornice 15* | Mortar (*opus reticolatum*), central wall, Augustan age |
| TM_10 | *Fornice 15* | Mortar (*opus reticolatum*), central wall, Julio-Claudian age |

The samples were then embedded in epoxy resin and, once polymerized, cut and polished to obtain thin sections for petrographic observation under a Polarized Optical Microscope (POM). Microchemical analysis was carried out by means of a Scanning Electron Microscope (SEM) used in backscattered electron (BSE) mode and coupled with an Energy-Dispersive Spectrometer (EDS).

POM investigations aimed to gather information on the textural and mineralogical features of the samples.

An examination of the aplastic inclusions and the aggregate fraction (i.e., monomineralic crystals and polymineralic lithic fragments in both cases) was conducted for the brick and mortar/plaster samples, respectively. In this regard, the granulometry, morphology, distribution, and packing of the inclusions were evaluated. In addition, the microstructure and the optical activity of the groundmass and the binder were described [27]. The binder/aggregate ratio and macroporosity (% area) were established in the mortar and plaster samples using standard comparison charts on images acquired by optical light microscopy [28]. Particular attention was given to the documentation of fractures, as well as primary and secondary macroporosity due to secondary alteration and degradation processes. The estimation of petrographic observations was conducted using a ZEISS Primotech TL/RL microscope equipped with an AxioCam ERc 5s Rev.2 camera to capture images.

The scanning electron microscope (SEM) analyses were conducted on carbon-coated cross-sections using an Ultra-High-Resolution SEM (UHR-SEM) ZEISS Cross Beam, following the instrumental conditions detailed below for image acquisition and EDS analysis, respectively: HV: 15 keV; probe current: 100 pA; working distance: 11 mm; image: BSE—SE-BSE signal; detector image: solid-state detector (SSD); Everhart–Thornley Detector (SE); and for EDS acquisition: HV: 15 keV; probe current: 100 pA; working distance: 12 mm; take-off angle: 40°; live time: 30 s.

The micro-chemical investigations provided a semi-quantitative estimation of the major chemical elements of the monomineralic grains and rock fragments within the samples, thus corroborating the optical microscopy examination [29]. Furthermore, the binder and groundmass chemical composition was analysed.

In the case of mortar and plaster layers, investigations were carried out to obtain information on the nature of the lime used as a binder. In this regard, a point analysis was performed on the core of the lime lumps within the samples. Their presence could be useful in providing information on the raw materials since their chemical composition is similar to that of the limestone used for the calcination process [30,31].

In order to determine the pozzolanic reactions that occurred between the aggregate fraction and the binder, several spot analyses were performed within the binder matrix as well (3 spot analyses for each analysed sample). Considering the atomic density of the analysed material, the actual size of the electron beam interaction spot is approximately 100–200 nanometres. Subsequently, the hydraulicity index (HI) of both the binder matrix and the lime lumps was calculated according to the following equation [32,33]:

$$\mathrm{HI} = \frac{SiO_2+Al_2O_3+Fe_2O_3}{CaO+MgO} \quad (1)$$

Higher HI values indicate a greater hydraulic character of the mixture, as this is associated with the presence of materials which display a high pozzolanic activity, leading to the formation of calcium (alumino)silicate hydrate (C-(A-)S-H).

## 4. Results and Discussion

### *4.1. Bricks*

The bricks used in the construction of the internal ambulatories of the theatre display a macroscopically homogeneous fabric and a light-yellow colour. They are approximately uniform in size and were carefully laid on a mortar bed, finished with a beaded jointing technique. The bricks are set within a cementitious core consisting of mortar and *caementa* made from crushed yellow brick, along with red and orange brick fragments arranged horizontally [20,26].

To investigate the compositional characteristics of the clay paste, a brick sample was collected from the innermost wall facing the *Ambulacro dei Cavalieri*.

Regarding the petrographic observations under POM, sample TM_2 exhibits a fabric characterized by a relatively homogeneous spatial arrangement and a serial size distribution of aplastic inclusions (Figure 3a). The latter are mainly fine-grained, with larger grains only sporadically observed. Inclusion sizes range from coarse silt (0.03–0.06 mm) to very coarse sand (1–2 mm). The packing, estimated using comparative charts, is moderate, corresponding to approximately 20% [34]. Regarding the mineralogical composition of the aplastic grains, monocrystalline quartz is the dominant monomineralic phase, while pyroxene crystals are rare (Figure 3b,c). Calcareous lithic fragments are commonly recognized among the rock grains, while scoriae fragments are sporadic. Additionally, a large fragment of quartzarenite with carbonate cement was identified in the sample (Figure 3d). The groundmass is moderately homogeneous, showing low-to-absent optical activity and common clay lumps. These lumps generally suggest incomplete maturation and/or mixing of the raw clay [27].

Porosity is low (<10%), with the predominant pore size class being <0.01 mm. Pores are partially filled with sparry calcite, precipitated within the pore network due to dissolution processes (Figure 3e). Perpendicular shrinkage cracks to the surface are also detected (Figure 3c).


(**a**) (**b**) (**c**)

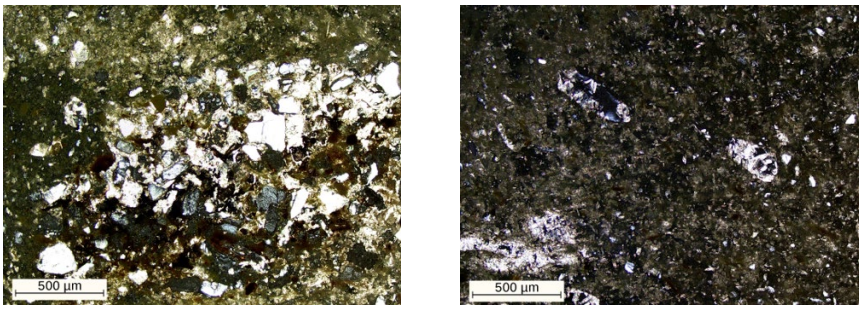


(**d**) (**e**)

**Figure 3.** Representative micrographs of the TM_2 brick sample showing (**a**) fabric characterized by a serial and homogeneous distribution of aplastic inclusions; (**b**,**c**) a pyroxene grain and a perpendicular shrinkage crack (red arrows); (**d**) large quartzarenite fragments with carbonate cement; (**e**) secondary calcite in the groundmass voids. Cross-polarised light acquisition was used for all the photomicrographs except for (**c**), captured with plane-polarised light. Legend: Px = pyroxene.

SEM morphological observations, together with EDS chemical micro-analyses, confirmed the preliminary observations made through POM. Additionally, spot analyses (spot size 100–200 nm) were conducted on the groundmass, with the corresponding EDS spectrum shown in Figure 4. The results reveal a composition quite rich in $SiO_2$ (45.9%) and $Al_2O_3$ (13.3%), along with smaller amounts of FeO (5.1%). Moreover, the high concentration of alkaline earth metals (MgO + CaO, 31.2%) can be attributed to the use of carbonate-rich clays. This might explain the light-yellowish coloration of the mixtures, although other factors linked to firing procedures and the kiln environment also contribute to the chromatic outcome and must be considered [35,36]. Further mineralogical analyses will be essential to fully understand and solve this aspect.

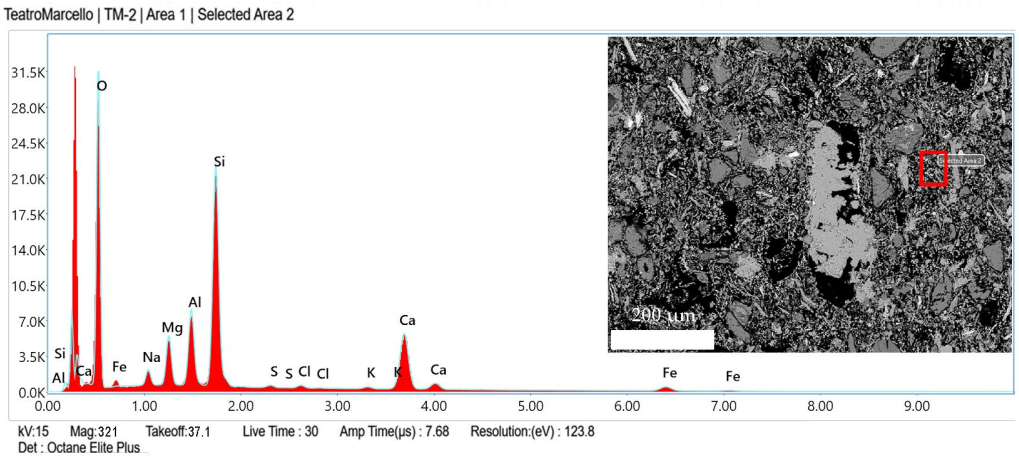


**Figure 4.** EDS micro-analysis on the clay groundmass of sample TM_2 and corresponding SEM-BSE image showing the spot analysis area (red square).

### *4.2. Mortars and Plasters*

#### 4.2.1. Minero-Petrographic Analysis

Minero-petrographic observation was conducted under POM on different plaster and mortar samples collected from diverse areas of the theatre.

1. *Mortars:*

As for the mortars of the *Theatrum Marcelli*, the petrographic analyses revealed textural and compositional characteristics that were similar across the investigated mortar samples.

The *Theatrum Marcelli* mortars consist of an aggregate fraction that is generally poorly sorted and exhibits a bimodal distribution, occasionally shifting towards a serial distribution. The distribution of the aggregate within the binder matrix ranges from moderately homogeneous to heterogeneous. Concerning the shape of the aggregate, it varies from angular to subrounded across all the analysed samples [37]. The packing is relatively high, ranging between 60 and 70%, and only rarely dropping to 50%. Overall, the aggregate size spans from medium sand (0.25–0.5 mm) to coarse sand (0.5–1 mm) and very coarse sand (1–2 mm), with samples frequently including finer fractions (0.125–0.25 mm) [38].

All the samples exhibit a mineralogical and petrographic composition that seems compatible with the potassium-rich incoherent pyroclastic deposits of the Roman Magmatic Province (Figure 5). In more detail, the aggregate is characterized by pozzolanic volcanic components, predominantly comprising leucitic tephrite and leucitite fragments (as *scoriae*) (Figure 5a–d). The latter generally show porphyritic to oligophyric textures, even though some highly porfiric individuals were observed. Within these *scoriae,* crystals of leucite (0.05–1.2 mm) (prevailing) and colourless–pale-green clinopyroxene (0.2–1 mm) are commonly recognized (Figure 5b). Leucite often displays a skeletal habit, resulting in a characteristic "star-like" morphology (Figure 5b–d,i). The groundmass appears reddish-brown with a variably vesiculated vitrophyric/criptocristallyne texture. Occasionally, some fragments lack any phenocrystals. Additionally, individual crystals of clinopyroxene, leucite, and, more rarely, biotite have been observed within the aggregate fraction. In terms of granulometry, samples TM_3 and TM_9 also contain two grains of leucitite and leucitic tephrite of larger dimensions characterized by a microcrystalline groundmass (Figure 5e).

On the whole, the volcanic aggregate exhibits mineral–petrographic and textural characteristics that appear analogous to those of the pyroclastic deposits from the Colli Albani volcano. Indeed, the eruptive products of the Colli Albani district display a silica-undersaturated and ultrapotassic composition, ranging from tephrite to foidite (leucitite) and tephriphonolite [11,12,39–42]. The dominant phenocryst phases mainly include leucite and clinopyroxene, some micas, and rare olivine, while the silica content is very low (<45 wt.%) [11,39]. The eruptive activity resulted in various successions of pyroclastic flows produced during different phases. The pozzolans used in Rome, mixed with lime to produce mortars with hydraulic properties, are actually the product of the final eruptive cycles of the Tuscolano–Artemisio phase (561–351 ka), characterized by a drier nature and associated with *Pozzolane Rosse* (460 ka), *Pozzolane Nere* (410 ka), and *Pozzolanelle* (355 ka) ignimbrites [41]. These deposits exhibit distinct petrographic and textural differences that allow their identification and differentiation in thin sections [13,43].

The optical observations of the aggregate of the *Theatrum Marcelli* mortars, with their distinctive, generally scarce porfiric index and the presence of colourless–pale-green clinopyroxene and leucite crystals (with prevailing skeletal star-like habits) within scoriae, suggest the use of the *Pozzolane Rosse* pyroclastic flow. In addition, the presence of *soriae* characterized by a higher porphyritic index is also found in the early explosive phase of the eruptive cycle [44].

The only noteworthy differences identified among the analysed samples regarding the aggregate fraction in terms of mineralogic phases include the presence of monocrystalline and polycrystalline quartz, feldspar, and trachytoid and chert lithic fragments in sample TM_4, alongside the volcanic components described above (Figure 5f). Moreover, sample TM_10 reveals a predominance of monomineralic phases, primarily consisting of clinopyroxene, feldspars, and biotite over *scoriae* (Figure 5g). In this case, the variability in the aggregate fraction components might be due to the different periods of execution of such mortars, which is attributable to a post-Augustan chronology (Julio-Claudian Age). Since feldspar is absent in the Alban Hills' volcanic products (it is rarely observed as a

microcrystal in the groundmass of some lavas) [39], it is probable that it derives from the air fall and colluvial ash deposits from the Monti Sabatini volcanic district (San Paolo Formation, about 437 ka), which stratigraphically overlies the *Pozzolane Rosse* unit and in which sedimentary quartz is also recognized [12].

Moreover, the presence of crushed ceramic fragments (*cocciopesto*) within mortar sample TM_1, taken from the *opus testaceum* wall inside the *Ambulacro dei Cavalieri*, could be seen as an attempt by the builders to produce an even more hydraulic and thus, durable, mixture. This is reasonable if we consider that these walls inside the *ambulacro* support the vaults of the *ima cavea* and are subject to quite humid conditions, promoted by the infiltration of meteoric water and facilitated by the numerous openings toward the seating tiers (*vomitoria* and basement windows) [26].

The binder matrix exhibits evident optical activity, with sub-rounded lime lumps of millimetric dimension frequently observed (Figure 5h). They show a peculiar porous and pelleted structure, which often shows clear internal shrinkage cracks [45,46]. Rare relicts of microfossils within the binder, likely residual and resulting from the rough calcination of the precursor limestone used to produce the lime, have also been observed. In all the analysed samples, clear reaction rims are evident at the interface between the binder and the aggregate, indicating the hydraulicization of the binder and the formation of hydrated phases (Figure 5i).

Porosity is very high, ranging from 20 to 30%, and comprises primary porosity, with predominantly subrounded pores, and secondary porosity, with irregular pores in the size ranges of 0.1–1 mm and >1 mm. Furthermore, the recrystallization of calcite, due to the dissolution phenomena of the binder, is observed within the pores.

The aggregate-to-binder ratio, determined using comparative charts, is quite variable, averaging at approximately 3:1, in agreement with Vitruvian recommendations [14]. However, a 1:1 ratio of pozzolanic aggregate/binder is also frequently observed, suggesting the use of variable raw material proportions, as documented in other Roman constructions [1,47–49].

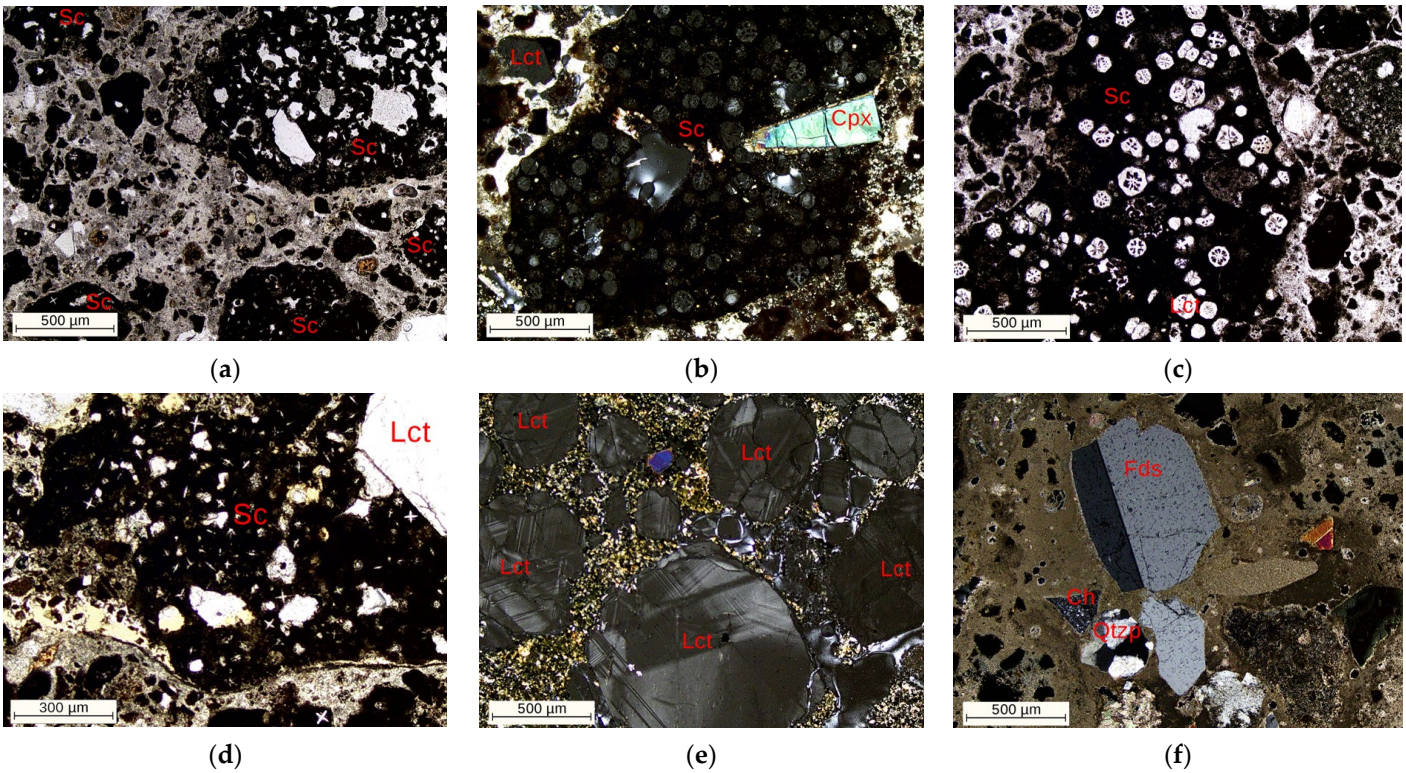

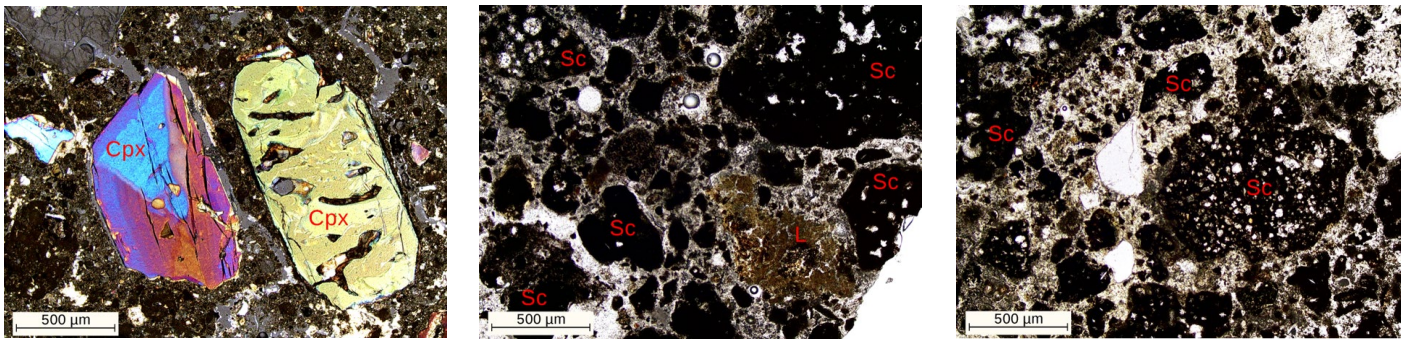


(**g**) (**h**) (**i**)

**Figure 5.** Microphotographs acquired during POM showing (**a**) volcanic *scoriae* constituting the aggregate fraction in sample TM_3; (**b**) a *scoria* in which both leucite and clinopyroxene crystals can be observed in sample TM_1; (**c**,**d**) leucite crystals with a characteristic skeletal, star-like habit in samples TM_7 and TM_6, respectively; (**e**) a large grain of leucitic tephrite in sample TM_3; (**f**) feldspar, polycrystalline quartz grains and a chert fragment in sample TM_4; (**g**) clinopyroxene crystals in sample TM_10; (**h**) a lump with internal shrinkage cracks in sample TM_7; (**i**) clear reaction rims surrounding volcanic *scoriae* in sample TM_1. Cross-polarized light acquisition was used for (**b**,**e**–**g**) photomicrographs, while (**a**,**c**,**d**,**h**,**i**) were captured with plane-polarized light. Legend: Sc = *Scoria*; Lct = leucite; Cpx = clinopyroxene; Fds = feldspar; Ch = chert; Qtzp = polycrystalline quartz; L = lump.

2. *Plasters*

As for the mortar samples, POM investigation was carried out on a plaster sample (TM_5) collected from the *ambulacro dei Cavalieri* (*fornice* 4). It revealed a stratigraphy composed of three distinct layers, differing in thickness and textural features.

The inner layer (Layer 1) (Figure 6a–c) is characterized by grains ranging from medium sand (0.25–0.5 mm) to coarse sand (1–2 mm). These grains exhibit a heterogeneous distribution and a bimodal sorting, with larger grains mixed with smaller ones. The packing is very low, at approximately 10%. In terms of the aggregate's composition, it includes sparse monomineralic crystals of monocrystalline quartz, pyroxene, and biotite, along with occasional *scoriae* grains. Lithic fragments of a carbonate nature, including marble and/or bioclasts (likely unburnt relicts of limestone after the process of calcination), are also identified. The binder, on the other hand, shows scarce optical activity with numerous lime lumps. Porosity is moderate, around 15%, and shrinkage cracks running parallel to the surface are also visible.

The intermediate plaster layer (Layer 2) (Figure 6a,d,e) exhibits a variable thickness (860–460 microns) and a discontinuous development on the underlying layer. The aggregate is quite uniformly distributed and ranges from coarse sand (0.5–1 mm) to fine sand (0.125–0.25 mm), also displaying bimodal sorting. It is characterized by monomineralic grains of clinopyroxene and lithic fragments, including trachytes, *scoria*, quartz arenites with ferruginous cement, and carbonate lithic fragments derived from the comminution of limestone and marble. The binder appears cryptocrystalline and the porosity, as in the inner layer, is moderate.

The upper layer (Layer 3) (Figure 6a) is thinner (700–400 microns) and consists exclusively of the binder.

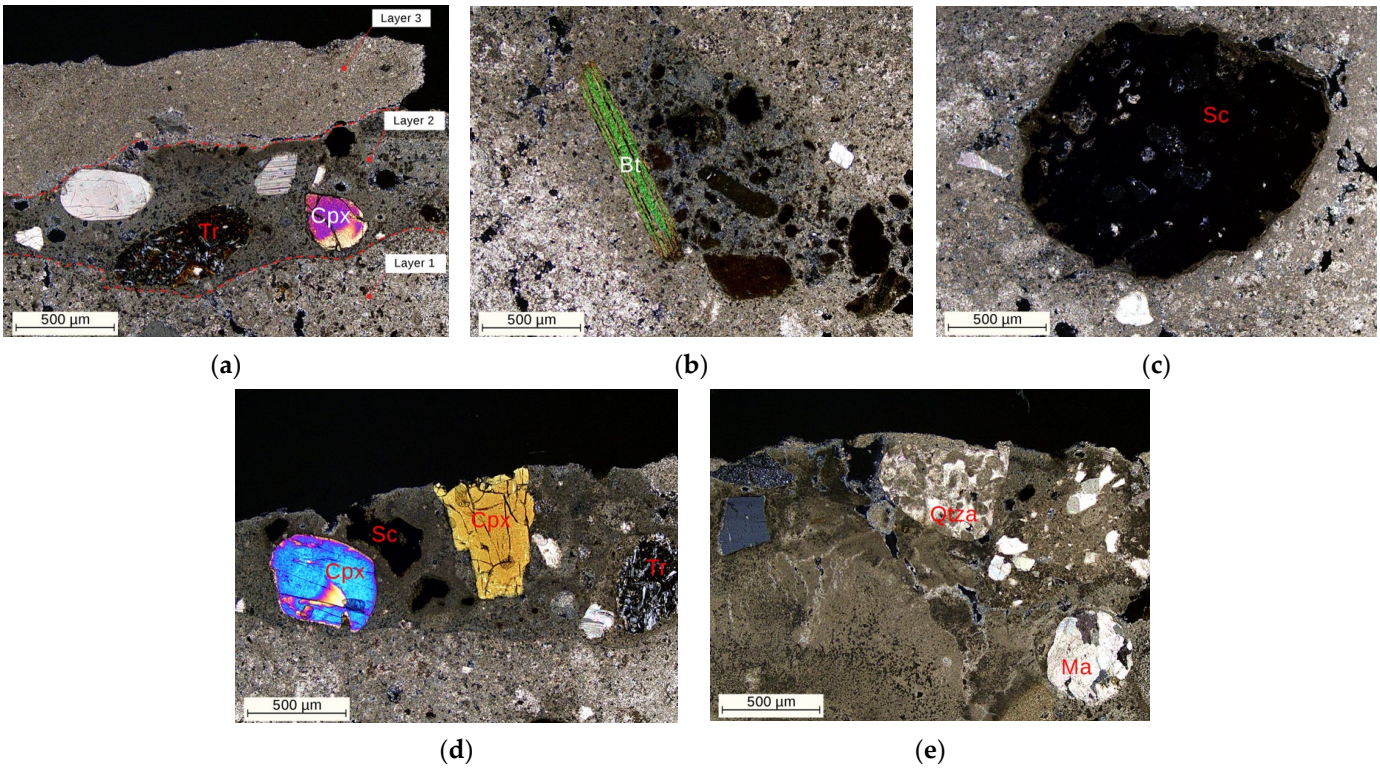


**Figure 6.** Representative micrographs of the TM_5 plaster sample showing (**a**) the stratigraphy consisting of the three different layers, highlighted by the red dotted lines; (**b**) a biotite crystal and (**c**) a *scoria* grain within Layer 1; (**d**) clinopyroxene trachyte grains; and (**e**) quartzarenites and carbonate lithic fragments inside Layer 2. Cross-polarised light acquisition was used for all the photomicrographs. Legend: Tr = trachyte; Cpx = clinopyroxene; Bt = biotite; Sc = *Scoria*; Qtza = quartzarenite; Ma = marble.

#### 4.2.2. SEM-EDS Investigation and HI Index

The semi-quantitative micro-chemical analyses were aimed at gaining a deeper understanding of the materials used as aggregates, obtaining information regarding the nature of the binder, and investigating the reactions between the binder and the aggregate.

For the characterization of the volcanic aggregate, SEM-EDS point analyses were conducted on clinopyroxene crystals within the examined samples. The results reveal compositional values that, as in the case of clinopyroxenes from the *Pozzolane Rosse* ignimbrite, fall within the diopside field of the QUAD diagram, exhibiting terms particularly enriched in calcium. Nevertheless, the comparison using main oxides is not successful in terms of establishing the provenance of deposits, because all clinopyroxenes of the Roman Volcanic Province fall more or less in the same compositional field (diopside–salite) [43,50].

Microchemical analyses were also carried out to investigate the composition of leucite crystals. The results from the SEM-EDS investigation reveal the presence of a zeolitic alteration process, with leucite crystals observed either as individual crystals or within the groundmass, often partially or completely replaced by analcime (Figure 7a–c). Analcime inclusions were also detected within the internal cavities of the grains (Figure 7b). Conversely, larger crystals appear generally fresh and unaltered (Figure 7a).

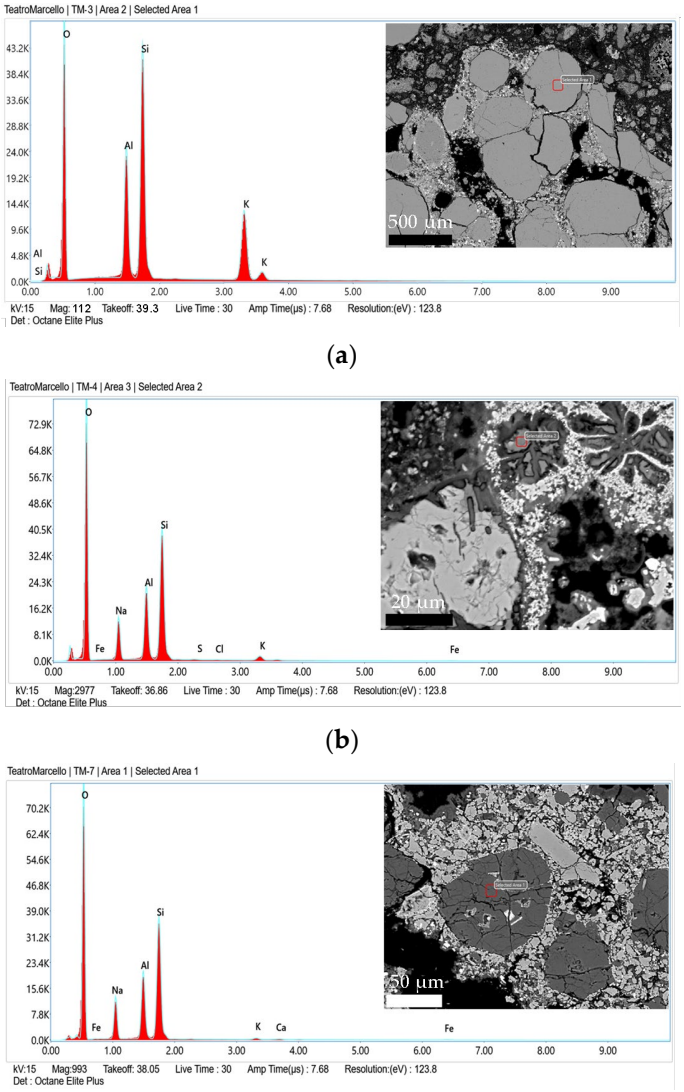


**Figure 7.** SEM-EDS investigations on leucite/analcime crystals detected within the aggregate of the plaster/mortar samples: (**a**) EDS spectrum of a fresh leucite crystal observed in sample TM_3 and corresponding SEM-BSE image showing the spot analysis area (red square); (**b**) EDS spectrum of some analcime inclusions inside the cavities of a leucite grain in sample TM_4 and corresponding SEM-BSE image showing the spot analysis area (red square); (**c**) EDS spectrum of a leucite crystal completely replaced by analcime in sample TM_7 and corresponding SEM-BSE image showing the spot analysis area (red square).

These features suggest the use of volcanic aggregate derived from intermediate alteration facies corresponding to the transitional Bt to Bw horizon of the *Pozzolane Rosse* marine isotope stage 11 paleosol, characterized by authigenic components formed through argillitic and zeolitic alteration [12]. These authigenic minerals, produced by specific weathering processes, exhibit a higher alkali content, which reacts with lime to form potassic-, sodic-, calcic-, alumina-, and ferric-calcium-silicate hydrates, surprisingly resulting in high-quality cements that remained durable even under extreme climatic conditions [12,15]. The minero-petrographic observations, together with the data obtained from the semi-quantitative EDS analyses, likely indicate the consistent use of volcanic ash comparable to *Pozzolane Rosse* eruptive products in the mortars and plasters of the *Theatrum Marcelli*. This finding is particularly significant, as it reveals that the *Theatrum Marcelli* construction represents a key expression of the evolution of Roman construction

techniques and mortar production technology, which would later form the foundation of the construction program adopted by Augustus. Indeed, it was only from the 1st century BCE, during the transition from the late Republican to the early Augustan period, that builders systematically improved the mechanical properties of mortars by selectively incorporating *Pozzolane Rosse* in the aggregate fraction. The presence of this type of pyroclastic deposit as an aggregate is observed for the first time in the mortars of Temple B in the Sacred Area of Largo Argentina, constructed after the fire of 111 BCE [10]. Previously, crushed fragments of tuff and volcanoclastic sediments from the San Paolo and Aurelia formations at the foot of the Capitoline Hill were commonly used [10]. These materials likely correspond to the *harenae cana* ("greyish in colour") described by Vitruvius, which, due to their earthy consistency and low compactness, formed the basis for poorly durable mortars [2]. In contrast, Vitruvius recommended volcanic sand ranging in colour from red (*rubra*) to black (*nigra*), which "makes a harsh, raspy, grating noise when rubbed vigorously in the hand", as the optimal choice. According to [2,12,13], this likely corresponds to the red and black pyroclastic deposits of the *Pozzolane Rosse*.

SEM-EDS chemical analyses also allowed us to conduct compositional studies of the binder used in the production of mortars and plasters. Table 2 shows the results of the SEM-EDS micro-chemical analysis with the corresponding HI calculated for both the binder and the lumps.

**Table 2.** Average values of the main oxides (wt.%) determined through SEM-EDS analysis on the binder (3 spot analyses for each sample) and on the lumps detected within the samples. TM_5$^{a}$: upper layer; TM_5$^{B}$: intermediate layer; TM_5$^{C}$: inner layer.

| Sample ID | Type | $Na_2O$ | MgO | $Al_2O_3$ | $SiO_2$ | S | Cl | $K_2O$ | CaO | FeO | HI |
|---|---|---|---|---|---|---|---|---|---|---|---|
| TM_1 | Binder | 0.6 | 7.8 | 1.8 | 6.8 | 0.5 | 0.0 | 0.5 | 81.9 | 0.0 | 0.096 |
| TM_3 | Binder | 0.5 | 0.3 | 4.9 | 14.5 | 0.5 | 0.4 | 1.4 | 77.7 | 0.0 | 0.248 |
| TM_4 | Binder | 0.5 | 6.3 | 2.0 | 6.9 | 0.4 | 0.0 | 0.8 | 83.0 | 0.0 | 0.100 |
| TM_5$^{a}$ | Binder | 1.5 | 2.7 | 1.0 | 2.7 | 0.6 | 0.5 | 1.8 | 73.8 | 0.0 | 0.040 |
| TM_5$^{b}$ | Binder | 1.8 | 4.6 | 3.5 | 12.1 | 1.5 | 1.0 | 1.8 | 73.8 | 0.0 | 0.199 |
| TM_5$^{c}$ | Binder | 0.5 | 2.7 | 0.4 | 3.8 | 0.6 | 0.5 | 0.1 | 91.5 | 0.0 | 0.045 |
| TM_6 | Binder | 1.2 | 0.3 | 4.3 | 13.7 | 1.0 | 1.3 | 1.1 | 77.4 | 0.0 | 0.231 |
| TM_7 | Binder | 0.6 | 2.3 | 5.0 | 9.6 | 0.7 | 0.2 | 2.1 | 79.4 | 0.0 | 0.179 |
| TM_8 | Binder | 0.0 | 0.8 | 4.3 | 12.0 | 0.8 | 0.3 | 0.9 | 80.9 | 0.0 | 0.200 |
| TM_9 | Binder | 0.0 | 0.6 | 4.7 | 13.7 | 0.6 | 0.4 | 0.7 | 79.3 | 0.0 | 0.230 |
| TM_10 | Binder | 0.2 | 0.3 | 2.8 | 8.2 | 1.9 | 0.4 | 0.5 | 85.7 | 0.0 | 0.128 |
| **Sample ID** | **Type** | **$Na_2O$** | **MgO** | **$Al_2O_3$** | **$SiO_2$** | **S** | **Cl** | **$K_2O$** | **CaO** | **FeO** | **HI** |
| TM_1 | Lump | 0.0 | 0.0 | 0.0 | 0.4 | 0.0 | 0.0 | 0.4 | 98.2 | 0.0 | 0.004 |
| TM_1 | Lump | 0.0 | 0.4 | 0.3 | 1.3 | 0.0 | 0.0 | 0.0 | 97.3 | 0.0 | 0.016 |
| TM_4 | Lump | 0.3 | 0.9 | 1.3 | 3.8 | 0.8 | 0.0 | 0.9 | 91.8 | 0.0 | 0.055 |
| TM_4 | Lump | 0.2 | 1.2 | 1.6 | 4.1 | 0.8 | 0.0 | 0.9 | 91.4 | 0.1 | 0.063 |
| TM_7 | Lump | 0.2 | 0.0 | 0.0 | 0.2 | 0.0 | 0.3 | 0.0 | 99.2 | 0.0 | 0.002 |
| TM_8 | Lump | 0.0 | 1.1 | 0.0 | 1.2 | 0.0 | 0.0 | 0.0 | 97.7 | 0.0 | 0.012 |

Point analyses (spot size 100–200 nm) of major elements carried out on lime lumps within the samples provided significant insights into the nature of the binder. The formation of these lumps is a topic widely debated in the literature. Their origin is believed to result either from the slaking of quicklime, caused by the use of the minimum amount of water sufficient to convert CaO into $Ca(OH)_2$ [51,52], or from inadequate and poor mixing of the aggregate and lime [53]. Other hypotheses link their formation to the maturation phase, during which a carbonate crust develops on the surface of the lime putty [54]. In any case, once they are formed, the lumps gradually convert into calcium carbonate due

to the carbonation process. As a result, these binder-related particles are fundamental for characterizing the raw materials used in mortar production, as their composition reflects that of their precursor limestone.

To minimize contamination from the aggregate, analyses were conducted on the innermost areas of the lumps. The results revealed a predominantly carbonate composition, with high CaO + MgO contents ranging from 92.6 wt.% to 99.2 wt.% and minor concentrations of $SiO_2$ + $Al_2O_3$ + $Fe_2O_3$. The hydraulicity index (HI) calculated for the lime lumps displayed very low values, between 0.002 and 0.063, indicating the aerial nature of the lime used in the production of all the analysed mixtures (HI < 0.10).

Similarly, point analyses were performed on homogeneous portions within the binder matrix to determine the hydraulicity index achieved through the addition of pozzolanic aggregate. EDS analyses revealed higher concentrations of $SiO_2$ + $Al_2O_3$ + $Fe_2O_3$ and lower CaO + MgO contents compared to those measured in the lime lumps. The hydraulicity index calculated for the binder fraction showed values ranging from 0.038 to 0.248. Specifically, samples TM_1, TM_4, and TM_10 fall within the range of feebly hydraulic limes (0.10 < HI < 0.16), while samples TM_3, TM_5 (intermediate plaster layer), TM_6, TM_7, TM_8, and TM_9 may be considered as averagely hydraulic limes (0.16 < HI < 0.31). Finally, in the upper and lower layers of sample TM_5, the values are comparable to those of aerial limes (HI < 0.10) (Figure 8).

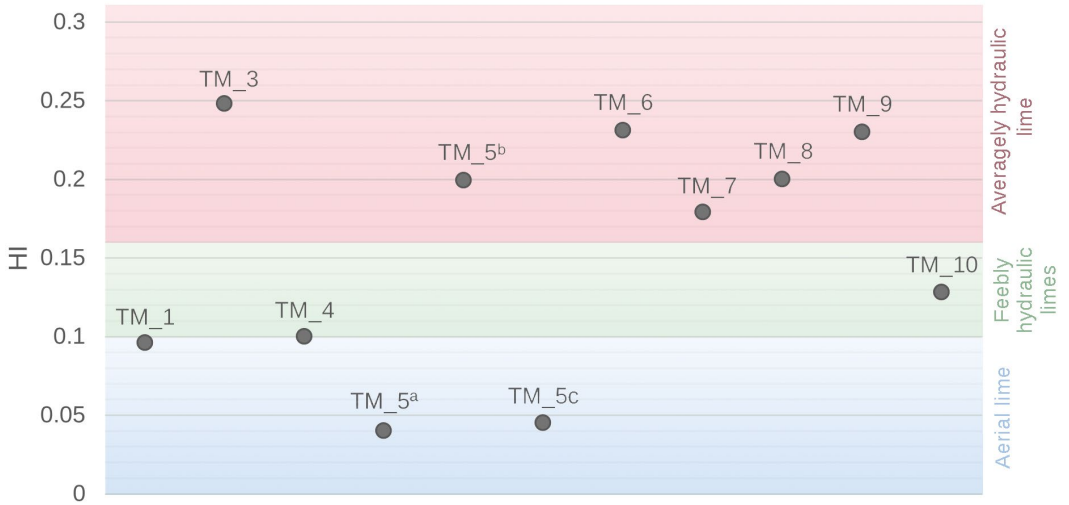


**Figure 8.** Graph showing the hydraulicity index (HI) values of the binder calculated for each sample and corresponding hydraulicity ranges. TM_5ᴬ: upper layer; TM_5ᴮ: intermediate layer; TM_5ᶜ: inner layer [32].

The results are in line with the traditional Roman preparation techniques of mortar/plaster pastes. The latter were indeed produced through the calcination of highly pure carbonate rock, thus resulting in a binder of a predominantly aerial nature. In this regard, it is well known that Roman builders primarily selected calcareous raw materials, mainly limestones quarried from Monte Soratte and the Monti Cornicolani, which on average exhibit a CaO content of 90% [13,55]. Thus, the lime in question lacked hydraulic properties, which were instead imparted to the mixture through the addition of volcanic aggregate [56–58]. This aggregate reacted with the hydrated lime to form cementitious hydration products. These compounds are clearly observable in the analysed samples, as they exhibit characteristic needle-like morphologies under SEM-BSE and a composition rich in silica, alumina, and alkali (Figure 9).

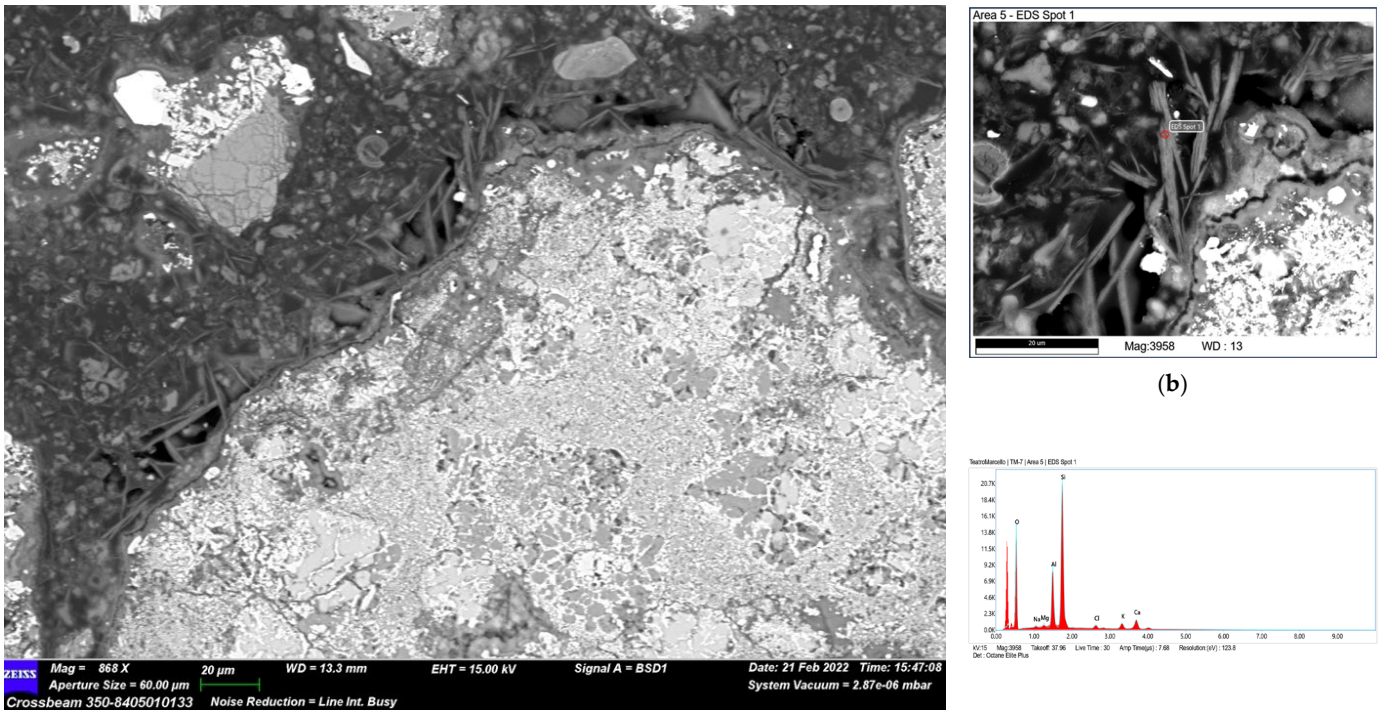


**Figure 9.** (**a**,**b**) SEM-BSE acquisitions of C-A-S-H phases at the interface between the *scoriae* and the binder in sample TM_7 showing peculiar needle-like morphologies and (**c**) corresponding EDS spectrum.

## 5. Conclusions

This diagnostic campaign conducted through complementary analytical techniques has provided valuable insights into the artificial stone materials (bricks, plasters, and mortars) used in the construction of the *Theatrum Marcelli*. The data obtained from petrographic and semi quantitative micro-chemical investigations not only allowed for the characterization of the raw materials, but also offered a deeper understanding of the production technology and the technological level achieved by early Imperial builders.

The bricks used in the internal ambulatories of the *Theatrum Marcelli* exhibit a homogeneous light-yellow fabric with fine-grained inclusions, predominantly quartz, and calcareous lithic fragments. The presence of a moderate concentration of alkaline earth metals (MgO + CaO) might suggest the use of carbonate-rich clays.

On the other hand, plasters and mortars were produced using raw materials with a relatively uniform composition. This confirms the typical "recipe" employed in the Roman era for making natural hydraulic mortars through adding pozzolanic material to lime. The pozzolanic component is mainly represented by leucitic tephrites and leucitites (as *scoriae*), as well as monomineralic grains of clinopyroxene, leucite, and rare biotite. This volcanic aggregate is consistent with ultrapotassic products from the Roman Magmatic Province, likely linked to the eruptive cycle of the Colli Albani volcanic district and comparable to the *Pozzolane Rosse* ignimbrites. The only compositional difference in the aggregate fraction among the analysed samples is the additional presence of monocrystalline and polycrystalline quartz, feldspar, trachytoid, and chert lithic fragments in sample TM_4, which may correspond to the air fall and colluvial ash deposits from the Monti Sabatini volcanic district that overlies the *Pozzolane Rosse*.

The presence of *Pozzolane Rosse* within the mortars/plasters of the *Theatrum Marcelli* highlights a key advancement in Roman construction techniques.

This practice, emerging during the transition from the late Republican to the early Augustan period, emphasizes the systematic improvement in mortar mechanical properties through the selective incorporation of *Pozzolane Rosse*. These findings position the *Theatrum Marcelli* as a significant case study in the evolution of Roman architectural technology, reflecting innovations that would later characterize the building program of Augustus.

**Author Contributions:** Conceptualization, M.F.L.R., F.M.A. and S.S.; methodology, L.R. and F.M.A.; formal analysis, L.R.; investigation, L.R., M.R., F.M.A., S.S. and M.A.Z.; resources, M.F.L.R.; data curation, L.R., M.R., F.M.A., S.S. and M.A.Z.; writing—original draft preparation, M.A.Z.; writing—review and editing, L.R., M.R., F.M.A. and M.A.Z.; supervision, M.F.L.R. and L.R. All authors have read and agreed to the published version of the manuscript.

**Funding:** This research received no external funding.

**Data Availability Statement:** Data is contained within the article or supplementary material.

**Conflicts of Interest:** The authors declare no conflicts of interest.

## References

1. Rispoli, C.; De Bonis, A.; Guarino, V.; Graziano, S.F.; di Benedetto, C.; Esposito, R.; Morra, V.; Cappelletti, P. The Ancient Pozzolanic Mortars of the Thermal Complex of Baia (Campi Flegrei, Italy). *J. Cult. Herit.* **2019**, *40*, 143–154. https://doi.org/10.1016/j.culher.2019.05.010.
2. Jackson, M.D.; Kosso, C.K. Scientia in Republican Era stone and concrete masonry. In *A Companion to the Archaeology of the Roman Republican Period*; Evans, J.D., Ed.; Wiley Blackwell: London, UK, 2013; pp. 268–284. https://doi.org/10.1002/9781118557129.ch17.
3. Jackson, M.D.; Marra, F.; Hay, R.L.; Cawood, C.; Winkler, E.M. The judicious selection and preservation of tuff and travertine building stone in Ancient Rome. *Archaeometry* **2005**, *47*, 485–510. https://doi.org/10.1111/j.1475-4754.2005.00215.x.
4. Jackson, M.D.; Kosso, C.; Marra, F.; Hay, R. Geological Basis of Vitruvius' Empirical Observations of Materials Characteristics of Rock Utilized in Roman Masonry, In *Proceedings of the Second International Congress of Construction History, Queens' College, Cambridge University, UK, 29 March 2006–2 April 2006*; Dunkeld, M., Campbell, J., Louw, H., Tutton, M., Addis, B., Thorne, R., Eds.; The Construction History Society: London, UK, 2006; Volume 2, pp. 1685–1702.
5. Collepardi, M. La lezione dei romani: Durabilità e sostenibilità delle opere architettoniche e strutturali. In Proceedings of the III Convegno AIMAT "Restauro E Conservazione Dei Beni Culturali: Materiali E Tecniche", Cassino, Italy, 3–4 October 2003.
6. Lancaster, L. *Concrete Vaulted Construction in Imperial Rome: Innovations in Context*; Cambridge University Press: Cambridge, UK, 2005.
7. Pavia, S. A petrographic study of mortar hydraulicity. In Proceedings of the HMC 08—1st Historical Mortar Conference, Lisboa, Portugal, 24–28 September 2008.
8. Rispoli, C.; Montesano, G.; Verde, M.; Balassone, G.; Columbu, S.; De Bonis, A.; Di Benedetto, C.; D'Uva, F.; Esposito, R.; Graziano, S.F.; et al. The key to ancient Roman mortars hydraulicity: Ceramic fragments or volcanic materials? A lesson from the Phlegrean archaeological area (southern Italy). *Constr. Build. Mater.* **2024**, *411*, 134408.
9. Gambino, F.; Glarey, A.; Cossio, R.; Appolonia, L.; d'Atri, A.; Borghi, A. SEM-EDS Characterization of Historic Mortar as a Tool in Archaeometric Study: An Updated Analytical Protocol Tested on the Roman Theatre of Aosta (NW Italy). *Archaeol. Anthropol. Sci.* **2022**, *14*, 179. https://doi.org/10.1007/s12520-022-01645-9.
10. Marra, F.; D'Ambrosio, E.; Gaeta, M.; Mattei, M. Petrochemical identification and insights on chronological employment of the volcanic aggregates used in ancient Roman mortars. *Archaeometry* **2016**, *58*, 177–200. https://doi.org/10.1111/arcm.12154.
11. Marra, F.; Danti, A.; Gaeta, M. The volcanic aggregate of ancient Roman mortars from the Capitoline Hill: Petrographic criteria for identification of Rome's "pozzolans" and historical implications. *J. Volcanol. Geotherm. Res.* **2015**, *308*, 113–126. https://doi.org/10.1016/j.jvolgeores.2015.10.007.
12. Jackson, M.; Deocampo, D.; Marra, F.; Scheetz, B. Mid-Pleistocene pozzolanic volcanic ash in ancient Roman concretes. *Geoarchaeol. Int. J.* **2010**, *25*, 36–74. https://doi.org/10.1002/gea.20295.
13. Jackson, M.; Marra, F.; Deocampo, D.; Vella, A.; Kosso, C.; Hay, R. Geological Observations of Excavated Sand (Harenae Fossiciae) Used as Fine Aggregate in Roman Pozzolanic Mortars. *J. Rom. Archaeol.* **2007**, *20*, 25–53. https://doi.org/10.1017/S1047759400005304.

14. Pollio, M.V. De Architectura. *The Architecture of Marcus Vitruvius Pollio*; Gwilt, J., Translator; Lockwood & CO.: London, UK, 1874. Available online: https://warburg.sas.ac.uk/pdf/kfh125b2128022.pdf (accessed on 28 November 2024).
15. Bencivenga, M.; Di Loreto, E.; Liperi, L. Il regime idrologico del Tevere, con particolare riguardo alle piene della città di Roma. In *Memorie Descrittive Della Carta Geologica D'Italia: La Geologia Di Roma*; VV. AA. Eds.; Istituto Poligrafico E Zecca Dello Stato: Rome, Italy, 1995; pp. 125–172.
16. Del Monte, M. La geomorfologia di Roma. In *La Geomorfologia Di Roma*; Sapienza Università Editrice: Rome, Italy, 2018; pp. 1–194.
17. Pantaloni, M.; Guerra, M.; Console, F.; Primerano, P. Rome before Rome: A River among two volcanoes. Discovering the relationship between the history of the city and the territory. *Geol. Field Trips Maps* **2023**, *15*, 1–66. https://doi.org/10.3301/GFT.2023.05..
18. Augustus, G.I.C.O. *Monumentum Ancyranum (Res Gestae Divi Augusti). Velleius Paterculus. Compendium of Roman History. Res Gestae Divi Augusti*; Shipley, F.W., Translator; Harvard University Press: Cambridge, MA, USA, 1924. Available online: https://penelope.uchicago.edu/Thayer/E/Roman/Texts/Augustus/Res_Gestae/home.html (accessed on 28 November 2024).
19. Tranquillus, C.S. De vita duodecim Caesarium.In *Lives of the Caesars*; Rolfe, J.C., Translator; Harvard University Press: Cambridge, MA, USA, 1914. Available online: https://penelope.uchicago.edu/Thayer/E/Roman/Texts/Suetonius/12Caesars/Julius*.html#44 (accessed on 28 November 2024).
20. Rossetto, P.C.; Buonfiglio, M. Teatro di Marcello: Analisi e riflessioni sugli aspetti progettuali e costruttivi. In *Arqueología De La Construcción II, Los Procesos Constructivos En El Mundo Romano: Italia Y Provincias Orientales (Atti Convegno Siena 2008)*; Camporeale, S., Dessales, H., Pizzo, A. Eds.; Madrid, Spain, 2010; pp. 51–70.
21. Dio, L.C.C. Historia Romana. Dio Cassius. In *Roman History, Volume VI: Books 51-55;* Cary, E., Foster, H.B., Translators; Harvard University Press: Cambridge, MA, USA, 1917. Available online: https://penelope.uchicago.edu/Thayer/E/Roman/Texts/Cassius_Dio/53*.html#30.6 (accessed on 28 November 2024).
22. VV. AA. Historia Augusta. In *Historia Augusta, Volume II: Caracalla. Geta. Opellius Macrinus. Diadumenianus. Elagabalus. Severus Alexander. The Two Maximini. The Three Gordians. Maximus and Balbinus*; Magie, D., Translator; Harvard University Press: Cambridge, MA, USA, 1924. Available online: https://penelope.uchicago.edu/Thayer/E/Roman/Texts/Historia_Augusta/Severus_Alexander/2*.html#44.7 (accessed on 28 November 2024).
23. Pensabene, P. Marmo ed evergetismo negli edifici teatrali d'Italia. Gallia e Hispania. *Malnake* **2007**, *29*, 7–52.
24. Gigli, F.; Pergola, S. Teatro di Marcello. Nuova campagna di rilievi, indagini e ricerche. *Bull. Comm. Arch. Rom.* **2023**, *124*, 330–341.
25. Hulsen, C. Il posto degli Arvali nel Colosseo e la capacità dei teatri di Roma antica. *Bachelor Commer.* **1894**, *22*, 312–324.
26. Buonfiglio, M. L'utilizzo dei laterizi nella costruzione augustea del Teatro di Marcello. In *Archeologia Dell'architettura, XX, 2015–Il Laterizio Nei Cantieri Imperiali. Roma E Il Mediterraneo. Atti Del I Workshop "Laterizio"(Roma, 27–28 Novembre 2014)*; Bukowiecki, E., Volpe, R., Wulf-Rheidt, U., Eds.; All'Insegna del Giglio: Florence, Italy, 2015; pp. 13–19.
27. Montana, G. Ceramic raw materials: How to recognize them and locate the supply basins—Mineralogy, petrography. *Archaeol. Anthropol. Sci.* **2020**, *12*, 175. https://doi.org/10.1007/s12520-020-01130-1.
28. Matthew, A.; Woods, A.; Oliver, C. Spots before the Eyes: New Comparison Charts for Visual Percentage Estimation in Archaeological Material. In *Recent Developments in Ceramic Petrology*; Middleton, A., Freestone, I., Eds.; British Museum Occasional Paper; British Museum: London, UK, 1991; pp. 221–263.
29. Janssens, K.; Van Grieken, R. *Non-Destructive Microanalysis of Cultural Heritage Materials*; Elsevier: Amsterdam, The Netherlands, 2005; pp. 80–82, ISBN 9780444559883.
30. Barba, L.; Blancas, J.; Manzanilla, L.R.; Ortiz, A.; Barca, D.; Crisci, G.; Miriello, D.; Pecci, A. Provenance of the limestone used in Teotihuacan (Mexico): A methodological approach. *Archaeometry* **2009**, *51*, 525–545. https://doi.org/10.1111/j.1475-4754.2008.00430.x.
31. Hughes, J.J.; Leslie, A.B.; Callebaut, K. The Petrography of Lime Inclusions in Historic Lime-Based Mortars. *Ann. Géol. Pays Hellén.* **2001**, *39*, 359–364
32. Boynton, R.S. *Chemistry and Technology of Lime and Limestone*; John Wiley & Sons, Inc.: New York, NY, USA, 1966.
33. Elsen, J.; Van Balen, K.; Mertens, G. Hydraulicity in Historic Lime Mortars: A Review. In *Historic Mortars*; Válek, J., Hughes, J.J., Groot, C.J.W.P., Eds.; RILEM Bookseries; Springer: Dordrecht, The Netherlands, 2012; pp. 125–139. https://doi.org/10.1007/978-94-007-4635-0_10.
34. Blair, T.C.; Mcpherson, J.G. Grain-size and textural classification of coarse sedimentary particles. *J. Sed. Res.* **1999**, *69*, 6–19. https://doi.org/10.2110/jsr.69.6.

35. Scatigno, C.; Prieto-Taboada, N.; Martinez, M.P.; Conte, A.M.; Madariaga, J.M. A non-invasive spectroscopic study to evaluate both technological features and conservation state of two types of ancient Roman coloured bricks. *Spectrochim. Acta Part A Mol. Biomol. Spectrosc.* **2018**, *204*, 55–63. https://doi.org/10.1016/j.saa.2018.06.023.
36. Fragnoli, P.; Boccalon, E.; Liberotti, G. Designing a 'yellow brick road' for the archaeometric analyses of fired and unfired bricks. *J. Cult. Herit.* **2023**, *59*, 231–246. https://doi.org/10.1016/j.culher.2022.12.007.
37. Powers, M.C. A new roundness scale for sedimentary particles. *J. Sediment. Res.* **1953**, *23*, 117–119. https://doi.org/10.1306/D4269567-2B26-11D7-8648000102C1865D.
38. Wentworth, C.K. A scale of grade and class terms for clastic sediments. *J. Geol.* **1922**, *30*, 377–392. https://doi.org/10.1086/622910.
39. Peccerillo, A. *Plio-Quaternary Volcanism in Italy*; Springer: Berlin/Heidelberg, Germany, 2005; ISBN 3-540-25885-X.
40. Trigila, R.; Agosta, E.; Currado, C.; De Benedetti, A.A.; Freda, C.; Gaeta, M.; Palladino, D.M.; Rosa, C. Petrology. In *The Volcano of the Alban Hills*; Trigila, R., Ed.; Università degli Studi di Roma "La Sapienza": Rome, Italy, 1995; pp. 95–165.
41. Conticelli, S.; Boari, E.; Benedetti, A.A.; Giordano, G.; Mattei, M.; Melluso, L.; Morra, V. Geochemistry, isotopes and mineral chemistry of the Colli Albani volcanic Rocks: Constraints on magma genesis and evolution. In *The Colli Albani Volcano*; Geological Society of London: London, UK, 2010; pp. 107–139. https://doi.org/10.1144/IAVCEI003.6.
42. Marra, F.; Deocampo, D.; Jackson, M.D.; Ventura, G. The Alban Hills and Monti Sabatini volcanic products used in ancient Roman masonry (Italy): An integrated stratigraphic, archaeological, environmental and geochemical approach. *Earth-Sci. Rev.* **2011**, *108*, 115–136. https://doi.org/10.1016/j.earscirev.2011.06.005.
43. Belfiore, C.M.; Fichera, G.V.; La Russa, M.F.; Pezzino, A.; Ruffolo, S.A.; Galli, G.D. A Multidisciplinary Approach for the Archaeometric Study of Pozzolanic Aggregate in Roman Mortars: The Case of Villa dei Quintili (Rome, Italy). *Archeometry* **2015**, *57*, 269–296. https://doi.org/10.1111/arcm.12085.
44. Freda, C.; Gaeta, M.; Giaccio, B.; Marra, F.; Palladino, D.M.; Scarlato, P.; Sottili, G. $CO_2$-driven large mafic explosive eruptions: The Pozzolane Rosse case study from the Colli Albani Volcanic District (Italy). *Bull. Volcanol.* **2011**, *73*, 241–256. https://doi.org/10.1007/s00445-010-0406-3.
45. Elsen, J.; Brutsaert, A.; Deckers, M.; Brulet, R. Microscopical study of ancient mortars from Tournai (Belgium). *Mater. Charact.* **2004**, *53*, 289–294. https://doi.org/10.1016/j.matchar.2004.10.004.
46. Elsen, J. Microscopy of historic mortars—A review. *Cem. Concr. Res.* **2006**, *36*, 1416–1424. https://doi.org/10.1016/j.cemconres.2005.12.006.
47. Columbu, S.; Lisci, C.; Sitzia, F.; Lorenzetti, G.; Lezzerini, M.; Pagnotta, S.; Raneri, S.; Legnaioli, S.; Palleschi, V.; Gallello, G.; et al. Mineralogical, Petrographic and Physical-Mechanical Study of Roman Construction Materials from the Maritime Theatre of Hadrian's Villa (Rome, Italy). *Measurement* **2018**, *127*, 264–276. https://doi.org/10.1016/j.measurement.2018.05.103.
48. Miriello, D.; Bloise, A.; Crisci, G.M.; de Luca, R.; de Nigris, B.; Martellone, A.; Osanna, M.; Pace, R.; Pecci, A.; Ruggieri, N. New compositional data on ancient mortars and plasters from Pompeii (Campania–Southern Italy): Archaeometric results and considerations about their time evolution. *Mater. Charact.* **2018**, *146*, 189–203. https://doi.org/10.1016/j.matchar.2018.09.046.
49. Jackson, M.D.; Logan, J.M.; Scheetz, B.E.; Deocampo, D.M.; Cawood, C.G.; Marra, F.; Vitti, M.; Ungaro, L. Assessment of material characteristics of ancient concretes, Grande Aula, Markets of Trajan, Rome. *J. Archaeol. Sci.* **2009**, *36*, 2481–2492. https://doi.org/10.1016/j.jas.2009.07.011.
50. Morimoto, N.; Fabries, J.; Ferguson, A.K.; Ginzburg, I.V.; Ross, M.; Seifert, F.A.; Zussman, J. Nomenclature of pyroxenes. *Mineral. Mag.* **1988**, *52*, 535–550. https://doi.org/10.1180/minmag.1988.052.367.15.
51. Hughes, J.J.; Cuthbert, S.; Bartos, P.J.M. Alteration textures in historic Scottish lime mortars and implications for practical mortar analysis. In Proceeding of the 7th Euroseminar on Microscopy Applied to Building Materials, Delft, The Netherlands, June 29-July 2 1999; pp. 417–426, ISBN 9076554021.
52. Callebaut, K.; Van Balen, K. Dry-Slaked Lime: An alternative binder for restoration mortars. In Proceedings of the International Workshop on Urban Heritage and Building Maintenance VII, Zürich, Switzerland, 1 September 2000; pp. 65–72.
53. Bakolas, A.; Biscontin, G.; Moropoulou, A.; Zendri, E. Characterization of the lumps in the mortars of historic masonry. *Thermochim. Acta* **1995**, *269–270*, 809–816. https://doi.org/10.1016/0040-6031(95)02573-1.
54. Bruni, S.; Cariati, F.; Fermo, P.; Cairati, P.; Alessandrini, G.; Toniolo, L. White lumps in fifth- to seventeenth-century A.D. mortars from Northern Italy. *Archaeometry* **1997**, *39*, 1–7. https://doi.org/10.1111/j.1475-4754.1997.tb00786.x.
55. Fichera, G.V.; Belfiore, C.M.; La Russa, M.F.; Ruffolo, S.A.; Barca, D.; Frontoni, R.; Galli, G.; Pezzino, A. Limestone provenance in Roman lime-volcanic ash mortars from the villa dei quintili, Rome. *Geoarchaeology* **2015**, *30*, 79–99. https://doi.org/10.1002/gea.21504.

56. Pavia, S.; Caro, S. An investigation of Roman mortar technology through the petrographic analysis of archaeological material. *Constr. Build. Mater.* **2008**, *22*, 1807–1811. https://doi.org/10.1016/j.conbuildmat.2007.05.003.
57. Belfiore, C.M.; Fichera, G.V.; Ortolano, G.; Pezzino, A.; Visalli, R.; Zappalà, L. Image processing of the pozzolanic reactions in Roman mortars via X-ray Map Analyser. *Microchem. J.* **2016**, *125*, 242–253. https://doi.org/10.1016/j.microc.2015.11.022.
58. Randazzo, L.; Ricca, M.; Ruffolo, S.; Aquino, M.; Davidde Petriaggi, B.; Enei, F.; La Russa, M.F. An Integrated Analytical Approach to Define the Compositional and Textural Features of Mortars Used in the Underwater Archaeological Site of Castrum Novum (Santa Marinella, Rome, Italy). *Minerals* **2019**, *9*, 268. https://doi.org/10.3390/min9050268.